

FEATURE ARTICLE

Attaching Organic Layers to Semiconductor Surfaces

Stacey F. Bent

*Department of Chemical Engineering, Stanford University, Stanford, California 94305**Received: August 2, 2001; In Final Form: November 28, 2001*

Methods that can be used to tailor the surface properties of semiconductors will become increasingly important as new applications for semiconductor-based materials continue to be developed. The attachment of organic groups in particular can impart new functionality to the surface, providing properties such as passivation, molecular recognition, lubrication, or biocompatibility. This article will focus on organic functionalization of Group IV surfaces using vapor phase delivery in a dry processing environment. A combination of experimental and theoretical methods has been applied to identify the bonding and reactivity of the organic layers at the semiconductor surface. The attachment chemistry of dienes and amines at the Si(100)- 2×1 surface will be described. We show that the [4+2] cycloaddition (Diels–Alder reaction) occurs readily for a range of conjugated dienes at the (100)- 2×1 surface of Si, and that the reaction occurs at the surfaces of Ge(100) and C(100) as well. In amine reactivity, competing reaction pathways such as N–H bond dissociation and dative bonding through the nitrogen lone pair have been observed. The potential for these different classes of attachment reactions to impact future applications will be discussed.

I. Introduction

Organic functionalization of semiconductors is emerging as an important growth area in the development of new semiconductor-based materials and devices. As the range of applications for semiconductor materials continues to expand, methods that can be used to tailor their surface properties become increasingly important. Organic modification is one means of providing new functionality to the semiconductor surface by depositing layers of organic molecules at the surface using either wet chemistry or vacuum based (dry) methods. The incorporation of organic materials at the surface offers scientists great flexibility in designing and creating unique molecular properties by tuning the nature of the organic groups. These properties may then be useful for providing new capabilities in optical, electronic, and mechanical function as well as in chemical and biological activity. Such hybrid organic/semiconductor materials are being explored for use in applications ranging from molecular electronics and computing to device implantation and biocompatibility, although at present time their use remains largely conceptual. Organic materials are also being incorporated increasingly in more conventional microelectronics processing, such as for next-generation dielectric materials for metal interconnect isolation.

Although a relatively new field, significant progress has already been made over the past few years both in developing useful methodologies for producing organic-modified semiconductor surfaces, and in achieving a detailed understanding of the forces that drive the attachment reactions at the surface. Both experimental and theoretical tools have been applied to investigate organic/semiconductor reactivity. Although most of the studies have focused on silicon surfaces, investigations of germanium, gallium arsenide, and even diamond have also been

performed. To date, the majority of the studies have looked at fundamental issues of bonding and attachment chemistry at the surface, and a great deal of insight has been gained concerning the nature of the semiconductor surface. The chemical knowledge obtained is providing the groundwork for the development of future applications.

This article will focus on studies that our group has performed over the past few years to investigate organic functionalization of the surfaces of Group IV solids. Our approach has been to use organic molecules containing reactive functionalities to form direct, covalent bonds to the surface in a dry processing environment. A goal is to deposit a closely packed monolayer of bifunctional molecules that react at the surface by only one of the functional groups, leaving available the other group for subsequent layering chemistry. At issue is the need to understand not only how each functional group reacts at the surface, but also how the reactions of different functional groups compete. A combination of experimental and theoretical methods has thus been applied to identify the bonding and reactivity of the organic layers at the semiconductor surface, and to interrogate the competition between various reactions. In this way we strive to ultimately develop the means by which to control the reactions.

A major theme of our research is to learn how to extend principles from organic chemistry to manipulate the reactions at semiconductor surfaces. The covalent nature of the Group IV semiconductor surfaces lends itself well to this type of analysis. Fundamentally, the interaction between organic molecules and semiconductor surfaces is localized and directional, a characteristic that makes the surface chemistry qualitatively different from catalytic reactions on metal surfaces. This covalent nature allows semiconductor surface reactivity to be well described within a molecular framework.

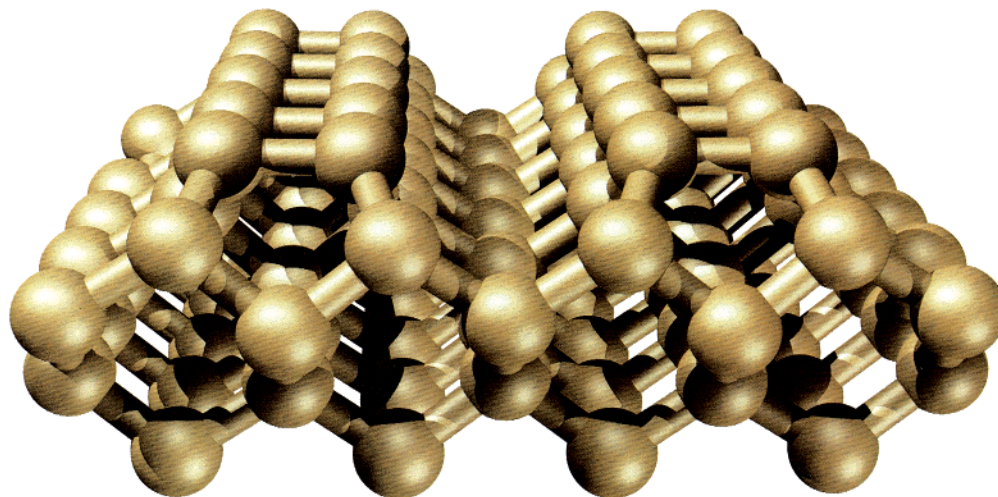


Figure 1. Illustration of the clean, reconstructed $(100)\text{-}2 \times 1$ surface characteristic of diamond, Si and Ge solids, containing rows of dimers. The buckling of the dimers is not shown.

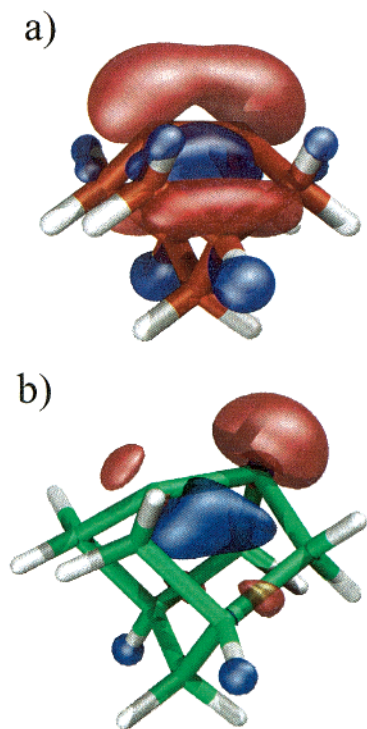


Figure 2. Orbital description (highest occupied molecular orbitals) for a (a) symmetric, and (b) tilted dimer. The orbitals were calculated from density functional theory using a C_9H_{12} cluster in (a) and a Ge_9H_{12} cluster in (b). The calculated tilt angle for a silicon dimer is intermediate between these two. [Figure modified from ref 159.]

For the industrially important (100) face of silicon, the surface atoms adopt a configuration that is conducive to a number of different attachment chemistries with parallels to organic reactions. The reconstructed $\text{Si}(100)\text{-}2 \times 1$ surface, illustrated in Figure 1, consists of rows of silicon dimers. The nature of these dimers is such that the silicon atoms are connected by a σ bond and a π -like interaction.^{1–3} An orbital description of a symmetric dimer is shown in Figure 2a. The π bond across the dimer is quite weak, yet a description of the Si–Si dimer bond as an analogue to a double bond provides a useful framework for describing the reactivity and properties of the dimer. The analogy between the Si–Si dimer and a double bond is shown to work particularly well for the class of attachment reactions known as cycloadditions. On the other hand, the weakness of

the π bond allows the dimers on $\text{Si}(100)\text{-}2 \times 1$ to tilt, as shown in Figure 2b. The resulting tilt imparts a zwitterionic-like property to the dimer, with the dimer characterized by one electron-deficient atom and one electron-rich atom in the dimer. This electronic property of the silicon surface opens up possibilities of using nucleophilic and electrophilic attachment reactions. Similar structures are formed for the Group-IV congeners $\text{Ge}(100)$ and $\text{C}(100)$.^{4–10}

Over the past few years, our studies, and those by a number of other groups, have revealed a rich chemistry between organic compounds and semiconductor surfaces in a vacuum. The work has led to a better understanding of how to describe and predict the reactivity of many important functional groups at the surface. In our laboratory, we have looked at many different reactive systems on clean silicon, and have also probed the functionalization reactions of several precursors on the germanium and diamond surfaces. In this paper, we have selected examples from two major classes of reactions—cycloaddition chemistry and amine chemistry—which illustrate the successful treatment of semiconductor surface reactivity through comparison to molecular analogues. The fundamental understanding gained in these studies is expected to impact a number of applications involving the integration of organic and semiconductor materials in the future.

The article is organized as follows. The following section describes the experimental and theoretical methods used to interrogate these systems. In section III.A, we develop the concept of cycloaddition chemistry as applied to surfaces, and in section III.B, we present studies identifying the Diels–Alder cycloaddition product in the reaction between butadiene and the $\text{Si}(100)\text{-}2 \times 1$ surface. Section III.C extends these studies to cyclic dienes at $\text{Si}(100)\text{-}2 \times 1$, and section III.D presents a comparative study of cycloaddition chemistry at the $\text{Ge}(100)$ and $\text{C}(100)$ surfaces. In section IV we examine the reactions of aliphatic amines at the $\text{Si}(100)\text{-}2 \times 1$ surface, including N–H bond cleavage and dative bond formation. In section V we present concluding remarks.

II. Experimental and Theoretical Methods

The principal tool in our studies of organic attachment reactions has been high resolution vibrational spectroscopy. Vibrational spectroscopy, especially when coupled with isotope labeling studies and *ab initio* quantum mechanical calculations, provides a powerful means of determining bonding of adsorbates

at the surface. Other methods also employed in these studies include near edge X-ray absorption fine structure spectroscopy and temperature-programmed reaction/desorption.

The studies were carried out in several different ultrahigh vacuum (UHV) apparatuses. Two chambers in our laboratory were used for studies of the Si and Ge surfaces. These systems have combined capabilities for infrared vibrational spectroscopy, temperature-programmed reaction/desorption (TPR/D), Auger electron spectroscopy (AES), and low energy electron diffraction (LEED).^{11,12} The chambers are equipped with ion guns for surface sputtering, and heating and cooling capabilities are present on the sample manipulators. The diamond IR experiments were performed in a UHV system at the Naval Research Laboratory, described elsewhere.¹³

All of the infrared measurements were performed in multiple internal reflection (MIR) mode using commercial Fourier transform infrared (FTIR) spectrometers. The single crystalline semiconductor samples were cut into a trapezoidal geometry of dimensions $1 \times 20 \times 50 \text{ mm}^3$ (Si or Ge) or $15 \times 3 \times 0.25 \text{ mm}^3$ (diamond), with 45° beveled edges. Infrared light from the FTIR spectrometer was focused through one of the beveled edges of the sample, undergoing multiple internal reflections from the two large crystal faces before being collected by a mirror and focused onto a HgCdTe (for Si or Ge) or InSb (for C) detector external to the chamber.

Different cleaning procedures were used for the silicon, germanium, and diamond samples. The Si samples were typically cleaned by sputtering with Ar^+ ions at room temperature followed by annealing to above 1020 K for 15–25 min. Subsequently, the sample was exposed to disilane (Si_2H_6) while cooling in order to prepare a smooth Si(100)- 2×1 surface.¹⁴ The Ge surface was cleaned by Ar^+ sputtering followed by thermal annealing to 875 K for 5 min.¹⁵ The diamond sample was prepared according to a procedure optimized at the Naval Research Laboratory. The procedure consisted of cleaning the sample in a sequence of acid mixtures,^{16,17} exposing it to a hydrogen microwave plasma to produce a smooth, hydrogen-terminated 2×1 reconstructed (100) surface, and then transferring it to the ultrahigh vacuum chamber where it was heated to 1310 K to remove the hydrogen.^{9,10} For all three surfaces, sample cleanliness and order were checked by Auger electron spectroscopy and LEED, or by monitoring the frequencies and line widths of the surface-hydride stretching peaks using infrared spectroscopy.

The near-edge X-ray absorption fine structure (NEXAFS) measurements were conducted on beamline U1 of the National Synchrotron Light Source (NSLS) at Brookhaven National Laboratory. A detailed description of the experimental end station apparatus has been given elsewhere.¹⁸ The resolution of the synchrotron monochromator was set at approximately 0.4 eV near the C K-edge region in the studies reported here.¹⁹

Both gaseous (1,3-butadiene, 1,3-butadiene-(2,3)- d_2 , 1,3-butadiene-(1,1,4,4)- d_4 , dimethylamine, and trimethylamine), and liquid (2,3-dimethyl-1,3-butadiene, cyclopentadiene, 1,3-cyclohexadiene, 1,4-cyclohexadiene, benzene, pyrrolidine, and *N*-methylpyrrolidine) reagents were used in these studies. Gaseous reagents were used without further purification. Liquid reagents were prepurified by at least three freeze–pump–thaw cycles before introduction into the reaction chamber. The purity of the compounds was verified in situ by mass spectrometry. Exposures are reported in units of Langmuir (L), where $1 \text{ L} = 10^{-6} \text{ Torr s}$. All exposures were performed by filling the chamber with the compound of interest for a set pressure and time. The pressures have not been corrected for ion gauge sensitivities.

The electronic structure calculations in this work are based on density functional theory (DFT)^{20,21} with Gaussian basis sets as implemented in the *Gaussian 98* suite of programs.²² The Si(100)- 2×1 and Ge(100)- 2×1 surfaces were modeled by a Si_9H_{12} and Ge_9H_{12} one-dimer cluster, respectively.^{23,24} All structures were fully optimized without geometrical constraints on the clusters. The structures of the stationary points on the potential energy surface were calculated at the BLYP/6-31G* level of theory.^{25,26} Single point energy calculations were performed on the optimized structures at the B3LYP level of theory^{26,27} with a split basis set scheme, in which the 6-311++G** basis set was used on the surface Si dimer atoms and the amine adsorbate, and the 6-31G* basis set was used on all the subsurface Si atoms and the terminating H atoms. The split basis set scheme serves to enhance the accuracy of the electronic structure of the chemically active atoms while minimizing computational costs. All B3LYP single-point energies reported are corrected by BLYP/6-31G* zero-point energies.

III. Attachment Reactions of Dienes at the Surface

A. Concepts in Cycloaddition Reactions: Extending Solution Chemistry to the Surface. The chemistry of organic molecules at a semiconductor surface is closely related to the surface electronic structure. The Si(100)- 2×1 surface, for example, consists of rows of dimers that are formed from the surface reconstruction (Figure 1).^{1–3} As described above, the dimers of the Si(100)- 2×1 surface contain two bonds between the two Si atoms: a strong σ -bond and a weak π -bond. Despite its low bond strength (estimated at 5–10 kcal/mol),^{2,28–31} the presence of the π bond is of sufficient magnitude to allow analogies to be drawn between the Si dimer and the alkene group in carbon chemistry. Alkenes are a well-studied functional group in organic chemistry, and reactions with alkenes form the basis of a significant group of synthetically useful reactions. It is therefore instructive to describe the reactivity of the Si(100)- 2×1 surface dimers in terms of the related alkene chemistry.

One important class of alkene chemistry are “cycloaddition” reactions. Cycloadditions are widely used in organic synthesis as a means of forming new carbon–carbon bonds and new carbon rings because of their versatility and high stereoselectivity.^{32–34} In a cycloaddition reaction, two π bonded molecules react to form a new cyclic molecule by the formation of two new σ bonds. The best known cycloaddition reaction is the Diels–Alder reaction, in which a conjugated diene reacts with an alkene, called the dienophile, to form a six-membered ring. The cycloaddition reactions are typically designated by the number of π electrons of each reactant molecule in the reaction, hence the Diels–Alder reaction is also known as the [4+2] reaction. Other cycloadditions include the [2+2] reaction (e.g., ethylene + ethylene) and the 1,3-dipolar cycloaddition reaction (e.g., ozone + ethylene).

Cycloaddition reactions are subject to the Woodward–Hoffmann selection rules. According to these rules, [2+2] cycloadditions are “symmetry forbidden” and should not occur without significant energy activation.³⁵ In organic solution chemistry, the [2+2] reaction is largely limited to synthesis involving photochemical activation. On the other hand, the [4+2] reaction is symmetry allowed, and consequently Diels–Alder reactions are commonly used in organic synthesis as a means of forming new C–C bonds and ring structures.^{32–34}

The earliest cycloaddition reactions studied at a semiconductor surface were reactions of simple alkenes and alkynes at the

Si(100)-2 \times 1 surface performed in the late 1980s.^{36–39} Although these reactions were not designated as such at the time, they fall into the category of [2+2] cycloaddition chemistry. For example, ethylene and propylene, as well as the related alkyne molecule acetylene, were reacted with the clean Si(100)-2 \times 1 surface in a vacuum in these and a number of more recent studies.^{23,36–64} The alkenes were found to chemisorb at room temperature, forming stable species that “bridge-bonded” across the silicon dimers on the surface. The reaction proceeded by loss of the π bond in the alkene and formation of two new Si–C σ bonds, hence the bonding was referred to as “di-sigma” bonding. Later studies determined that the dimer bond remains intact in this reaction.^{48–50,54,56–59,61–64} In the context of cycloaddition chemistry, the four-membered disilacyclobutane-like (Si_2C_2) reaction product can be labeled as the [2+2] cycloaddition product. Although this reaction formally is symmetry forbidden and is slow for the analogous homogeneous reaction,^{33,35} the surface [2+2] cycloaddition reaction appears to be facile, occurring readily with most alkenes at room temperature.⁶⁵ It has been proposed that the reaction occurs at the silicon surface by an asymmetric reaction pathway that lowers the reaction symmetry and results in little or no energetic barrier.^{48,51,60,66} The symmetry rules may be relaxed by the dynamic tilting of dimers at room temperature, combined with the relative weakness of the π bond.

The product of the [2+2]-like reaction is a tightly bonded organic group, directly attached to the silicon surface through two strong Si–C bonds (~ 82 kcal/mol each).⁶⁷ Consequently, [2+2] cycloaddition has attracted interest as a method by which to functionalize the Si(100)-2 \times 1 surface. Subsequent studies over the past several years have looked at more complex unsaturated hydrocarbons, and to date a range of alkenes, including benzene and its derivatives,^{68–87} cyclopentene,^{88–92} cyclohexene,^{83,93,94} cyclohexadiene,^{83,92,93,95} and cyclooctadiene^{90,96–98} have been probed.

In systems such as ethylene/Si(100)-2 \times 1, chemisorption occurs by *direct addition*, i.e., interaction of one olefinic group with a silicon dimer. In 1997, an alternative reaction scheme—*conjugate addition* reaction between silicon dimers of Si(100)-2 \times 1 and dienes—was proposed by Konecny and Doren.⁹⁹ In particular, they calculated that the silicon dimers would serve as dienophiles toward dienes in the Diels–Alder [4+2] cycloaddition reaction, leading to the formation of a six-membered Si_2C_4 ring. The calculations showed that there is a substantial thermodynamic driving force (54 kcal/mol) to form the product of a [4+2] reaction between cyclohexadiene and the silicon dimer, modeled using a Si_9H_{12} one-dimer cluster. This is significantly more energy than is gained in the competing [2+2] reaction (39 kcal/mol) involving only one of the double bonds; the increased stability of the [4+2] product was attributed to reduced ring strain in the six-membered ring product. In addition, the calculations predicted that the reaction should occur with little or no energetic barrier, consistent with the Woodward–Hoffmann rules for a [4+2] reaction.^{23,66,99} Subsequent theoretical calculations by a number of groups^{66,67,100} have confirmed the energetic favorability of the [4+2] cycloaddition reaction not only on Si(100)-2 \times 1, but also on Ge(100)-2 \times 1 and C(100)-2 \times 1.

B. Butadiene/Si(100)-2 \times 1. Studies carried out in our laboratory provided the first experimental evidence for the proposed Diels–Alder reactions with the Si(100)-2 \times 1 surface. Butadiene was chosen as a prototypical conjugated diene for these studies. In principle, butadiene can react either by direct [2+2] addition through one of its double bonds, or by Diels–

Alder [4+2] cycloaddition involving both double bonds. Figure 3 shows MIR–FTIR spectra of 1,3-butadiene chemisorbed on Si(100)-2 \times 1 at room temperature (Figure 3a) and physisorbed at low temperature (Figure 3b), along with the corresponding spectra of two deuterium-labeled isotopes (Figure 3c–f). Subsaturation exposures (verified by Auger electron spectroscopy) at room temperature were used to avoid the possibility of intermolecular interactions.

As evident in Figure 3, 1,3-butadiene adsorbed at room temperature shows two primary absorption features at 2994 cm^{-1} and near 2895 cm^{-1} . No significant Si–H stretch was observed in the spectrum, supporting the absence of C–H bond dissociation. The peaks that are observed are consistent with olefinic and aliphatic C–H stretches. Neither the peak at ~ 3080 cm^{-1} , which is one of the most intense features in the spectrum of physisorbed 1,3-butadiene multilayers, nor any other features corresponding to a terminal $=\text{CH}_2$ group (usually observed above 3020 cm^{-1}), are seen within the signal-to-noise level in the chemisorbed butadiene spectrum. This result is significant because the product of a [2+2] reaction between one alkene group in butadiene and the Si dimer would retain a terminal $=\text{CH}_2$ group that should yield an absorption feature in the region near 3080 cm^{-1} . Instead, the observed spectrum is in closest agreement with the structure corresponding to the Diels–Alder adduct (shown in inset to Figure 3), where the olefinic C–H groups are internal to the ring.

The complementary studies of the deuterated butadienes provide further support for this spectroscopic assignment. In Figure 3c, the spectrum of 1,3-butadiene-(1,1,4,4,)- d_4 chemisorbed on Si(100)-2 \times 1 at room temperature exhibits a single absorption feature in the C–H stretch region, at 2989 cm^{-1} , while that of 1,3-butadiene-(2,3)- d_2 (Figure 3e) shows a broad feature near 2900 cm^{-1} . The broad absorption feature centered near 2895 cm^{-1} observed for the nondeuterated 1,3-butadiene adsorbed at room temperature can therefore be assigned to the terminal CH_2 groups in butadiene. The absorption frequency of the stretching modes for these CH_2 groups is too low to originate from sp^2 -hybridized carbon, confirming the loss of the 1,3-double bonds in butadiene as occurs in the Diels–Alder product.

NEXAFS spectroscopy provides a complementary technique for probing the bonding of organic layers at single crystalline semiconductor surfaces, and it can yield accurate information about structure and orientation of surface intermediates. To further investigate the Diels–Alder product at the Si(100)-2 \times 1 surface, NEXAFS measurements were undertaken of a related diene, 2,3-dimethyl-1,3-butadiene. As for 1,3-butadiene, infrared studies of 2,3-dimethyl-1,3-butadiene had also indicated formation of the Diels–Alder product for this compound.¹⁰¹

Figure 4 presents NEXAFS spectra of this molecule on a Si(100)-2 \times 1 surface taken at 100 K and at 300 K. The spectra in Figures 4a,b for multilayer and submonolayer films at 100 K exhibit 4 π^* transitions in the NEXAFS spectra.¹⁰² The presence of these four transitions and their relative spacings are consistent with the presence of two π^* orbitals with different energies (a consequence of conjugation), and the possibility of transition to these two π^* orbitals from two core levels with different energies (a consequence of the inequivalency of the core levels of the carbon atoms in the 1 and 4 vs 2 and 3 positions.) Hence, the spectra are indicative of unreacted (physisorbed) 2,3-dimethyl-1,3-butadiene. The spectrum of submonolayer exposure of 2,3-dimethyl-1,3-butadiene chemisorbed on Si(100)-2 \times 1 at 300 K is presented in Figure 4(c).

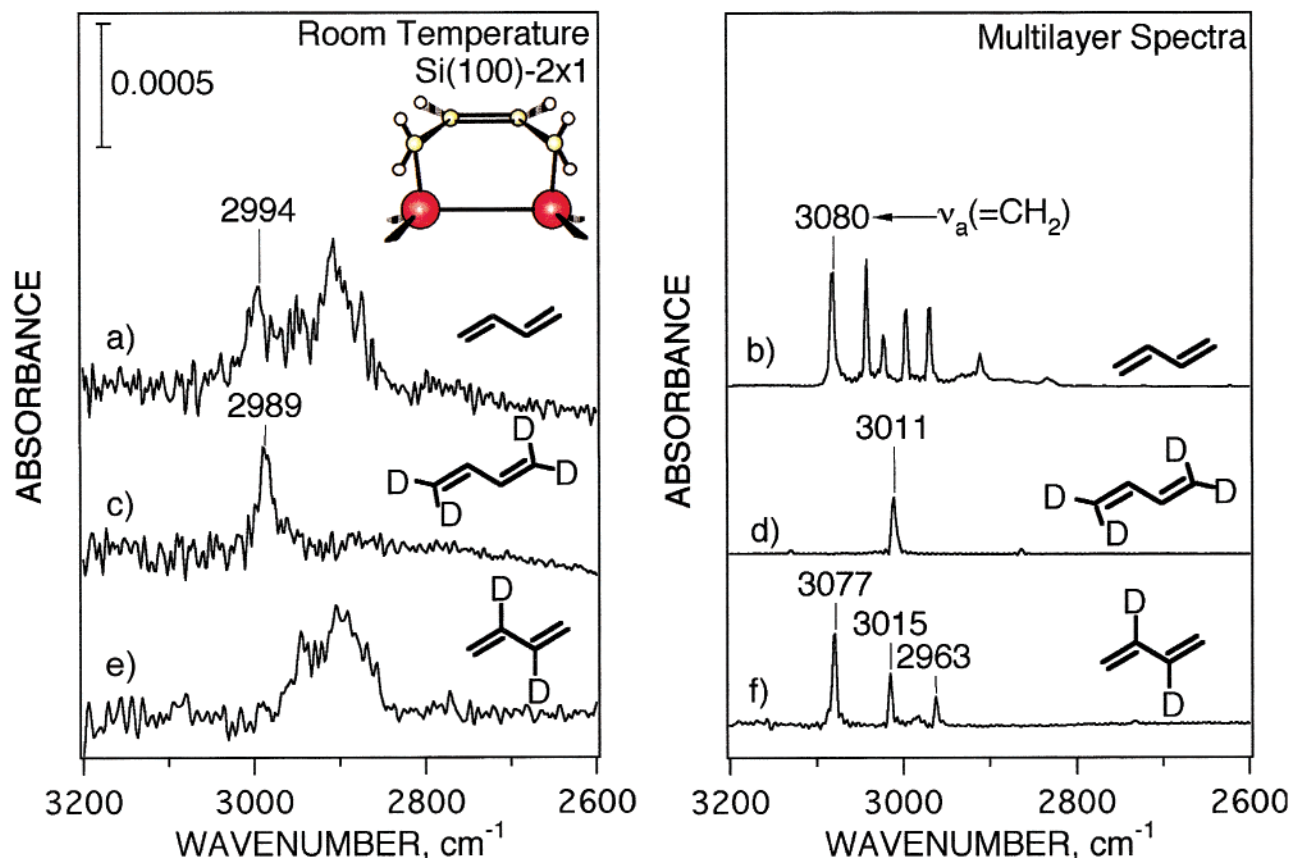


Figure 3. Infrared spectra of 1,3-butadiene adsorbed on a Si(100)- 2×1 surface: (a) 1 L of 1,3-butadiene adsorbed at 300 K, (b) multilayers of 1,3-butadiene at 100 K, (c) 1 L of 1,3-butadiene-(1,1,4,4)- d_4 adsorbed at 300 K, (d) multilayers of 1,3-butadiene-(1,1,4,4)- d_4 adsorbed at 100 K, (e) 1000 L of 1,3-butadiene-(2,3)- d_2 adsorbed at 300 K, (f) multilayers of 1,3-butadiene-(2,3)- d_2 adsorbed at 100 K.

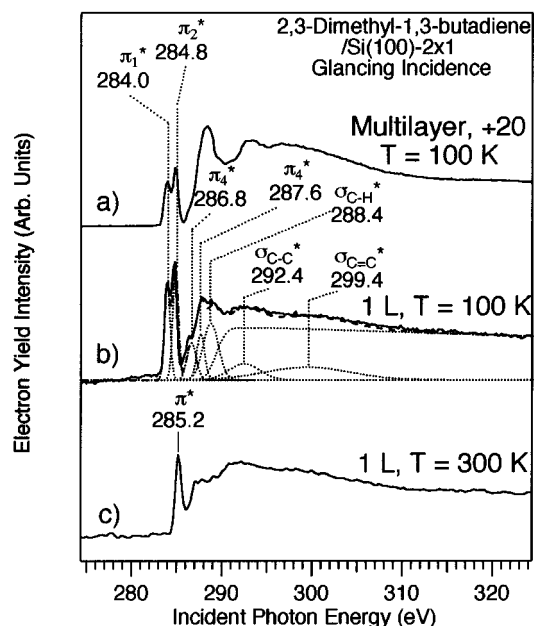


Figure 4. NEXAFS spectra of 2,3-dimethyl-1,3-butadiene on Si(100)- 2×1 obtained at glancing incidence of the incoming photon flux. (a) Multilayers physisorbed at 100 K. (b) Submonolayer (1 L) physisorbed at 100 K. (c) Submonolayer (1 L) chemisorbed at room temperature. [Reprinted with permission from ref 101. Copyright 1998 American Institute of Physics.]

Only one π^* transition is present in the 300 K spectrum and its energy is significantly higher than that of the π^* transitions in the physisorbed 2,3-dimethyl-1,3-butadiene. The energy of this π^* transition is consistent with the π^* transitions in mono-

unsaturated compounds,¹⁰² indicating that the π conjugation is lost. Although a unique assignment is not possible, the spectrum is in accordance with the structure of the Diels–Alder adduct.

In addition to information on chemical state, NEXAFS spectroscopy was used to determine the bonding geometry of chemisorbed 2,3-dimethyl-1,3-butadiene through polarization dependent studies. An analysis of data obtained at different incident angles of the incoming photon beam¹⁰² indicates that the angle between the π^* transition moment and the surface normal is $41 \pm 2^\circ$. This is in fair agreement with the theoretical prediction by Konecny and Doren, who calculated the angle between the double bond in this intermediate and the silicon surface plane to be 30° .^{23,99} The small discrepancy between experiment and theory may be due to the influence on the bonding angle of adjacent dimers at the surface, an effect which is absent in the 1-dimer cluster calculations.¹⁰³ Alternatively, the discrepancy may arise from the presence of a side product with different geometry,¹⁰⁴ an effect that would introduce an error into the experimental angle determination. Subsequent investigations of this system also suggested the presence of a side product of the Diels–Alder reaction of butadiene on Si(100)- 2×1 . STM studies showed the side product to be present in about 20% yield. Hovis et al. assigned this species to a [2+2] adduct based on a very small 3080 cm^{-1} peak in the infrared spectrum.¹⁰⁴ However, Doren et al. have proposed based on a theoretical analysis that the side product observed in STM may be one in which butadiene bridges silicon atoms from two adjacent dimers.¹⁰⁵

Studies were also undertaken to investigate the thermal stability of the Diels–Alder adduct at elevated temperatures. For both dienes studied, decomposition, rather than molecular

desorption, is found to be the dominant pathway at elevated temperatures. In temperature programmed desorption spectra, only a small amount of molecular butadiene desorption from Si(100)-2 \times 1 is observed, and no desorption of any other hydrocarbon or hydrocarbon fragment was found.¹⁰¹ Desorption of H₂ is observed at 780 K, consistent with loss from monohydride species. These results indicate that the major reaction pathway for both 1,3-butadiene and 2,3-dimethyl-1,3-butadiene chemisorbed on a Si(100)-2 \times 1 surface is complete dehydrogenation to form surface carbon and Si-H, which upon further heating leads to the recombinative desorption of H₂ at temperatures near 800 K. AES studies show that within experimental uncertainty the same coverage of carbon exists on the surface before and after desorption.

In summary, the results of MIR-FTIR and NEXAFS studies show that both 1,3-butadiene and 2,3-dimethyl-1,3-butadiene react with the Si(100)-2 \times 1 surface to form the Diels-Alder adduct as the major product at room temperature. In this reaction, the silicon dimer at the surface acts as a dienophile, analogous to a Si=Si or C=C double bond in molecules, implying that a covalent (molecular) description of the silicon dimer is appropriate to interpret the conjugate addition reaction. The thermal studies suggest that decomposition is the major pathway after chemisorption on a Si(100)-2 \times 1 surface at room temperature, but that a small fraction of molecules, probably on the order of few percent, desorbs molecularly. This is in contrast to the behavior in solution, where many Diels-Alder reactions are reversible. The results presented above clearly indicate that the interaction of butadienes with a Si(100)-2 \times 1 surface at room temperature results in chemisorption of these hydrocarbons to form strongly bound species.

C. Cyclic Dienes/Si(100)-2 \times 1. Butadienes served as the starting point for investigating the [4+2] reaction on Si(100)-2 \times 1. Motivated by this work, subsequent studies by our group and others have shown that other dienes can also be reacted in similar fashion. Cyclic dienes in particular may provide a good choice for a multistep functionalization process because the rigidity of the rings may add additional mechanical and thermal stability to the first layer.¹⁰⁶

We have investigated the reactivity of several other cyclic dienes, including cyclopentadiene,¹⁰⁷ 1,3- and 1,4-cyclohexadiene,⁸³ and benzene.⁷³ On the bases of the results from solution-phase organic chemistry, the propensity of each of these dienes to undergo Diels-Alder chemistry would be expected to differ significantly between molecules. For example, while cyclopentadiene and 1,3-cyclohexadiene are conjugated dienes that might be expected to react like butadiene with the surface, 1,4-cyclohexadiene is not conjugated and hence would not be expected to undergo the Diels-Alder reaction. Furthermore, benzene, with significant aromaticity energy, is not an efficient Diels-Alder reagent in organic chemistry and rarely undergoes Diels-Alder reactions in solution phase.

Indeed, differences in product distributions were found to exist for the surface reaction of the various cyclic dienes. However, for all the conjugated dienes that we examined (cyclopentadiene, 1,3-cyclohexadiene, and benzene), we have found evidence for at least some significant formation of the Diels-Alder product at the Si(100)-2 \times 1 surface.

Cyclopentadiene, which is well-known for its high reactivity in Diels-Alder reactions (as exemplified by the spontaneous dimerization of the molecule in neat solution to form dicyclopentadiene via an intermolecular Diels-Alder reaction), was determined by a combination of infrared spectroscopy and theoretical calculations to form primarily the Diels-Alder

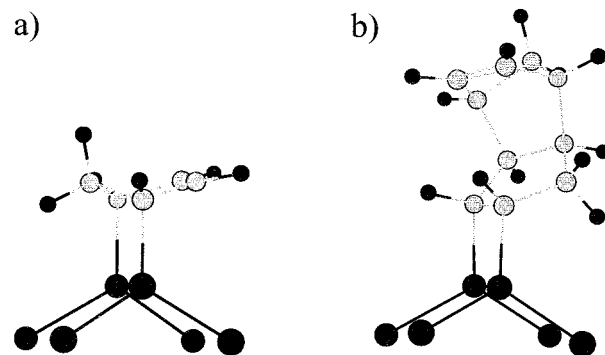


Figure 5. Energy minimized adsorption configurations for (a) the [4+2] cycloaddition product of cyclopentadiene with Si(100)-2 \times 1 and (b) one of the [2+2] cycloaddition products of dicyclopentadiene with Si(100)-2 \times 1.

product.¹⁰⁷ Interestingly, studies showed that the saturation coverage of cyclopentadiene at the Si(100)-2 \times 1 surface was less than 65%, whereas its dimer, dicyclopentadiene, which forms the [2+2] cycloaddition product, fills 30–40% more of the surface than cyclopentadiene. The difference may be the result of the different adduct geometries for the [4+2] versus [2+2] product. The geometries as calculated by DFT methods are shown in Figure 5. Whereas the Diels-Alder product tilts at an angle away from the surface normal (similar to the angle measured by NEXAFS for 2,3-dimethylbutadiene), the four-member ring formed in the [2+2] reaction is more aligned with the surface normal. For certain configurations of dicyclopentadiene, the [2+2] adduct may be able to pack with higher density at the surface.¹⁰⁷ This result suggests the possibility that lower saturation coverages may be achieved in general for the Diels-Alder product due to the tilt angle of the six-membered ring; however, further studies are necessary before such conclusions can be reached.

Studies of 1,3-cyclohexadiene also present evidence for formation of the Diels-Alder product, although infrared and NEXAFS data, together with the results of a previous study,¹⁰⁴ reveal the presence of [2+2] or other surface products as well.⁸³ The unconjugated 1,4-cyclohexadiene also adsorbs on Si(100)-2 \times 1, presumably by [2+2] cycloaddition, yielding an infrared spectrum that differs from that for 1,3-cyclohexadiene. TPD studies show that upon heating, both cyclohexadienes undergo partial dehydrogenation to evolve benzene, along with some molecular desorption of the parent molecule and some further decomposition/dehydrogenation. Annealing IR studies of chemisorbed 1,3-cyclohexadiene indicate that decomposition of the molecule occurs over the temperature range of 400–600 K. This observation of decomposition of the organic layer at 100–200 °C above room temperature is typical for the cycloaddition systems that we have studied on Si(100)-2 \times 1. While it signifies a reasonable thermal stability for the organic/semiconductor systems, it does provide limitations for the temperatures at which further processing of the materials can be performed.

Benzene formed the most complex product distribution of the C₆-cyclic dienes. A number of methods by different investigators have now been brought to bear on the benzene/Si(100)-2 \times 1 system, and the body of data obtained indicate that multiple bonding configurations are formed.⁶⁵ Some of these adsorption structures are metastable and convert to other structures as a function of time (or temperature). One of the bonding configurations is the Diels-Alder product, which converts in time to a bridge bonded structure in which the benzene molecule bonds to two adjacent dimers in the dimer

row. Each of the bonding configurations that are observed breaks the aromaticity of the benzene ring. However, the new bonds formed to the surface are sufficiently strong to make the adsorption reaction significantly exothermic despite this energy loss.

D. Butadiene/Ge(100) and C(100). It is intriguing that the analogue of a key reaction in organic chemistry, e.g., the Diels–Alder reaction, occurs across the silicon dimer on the Si(100)-2 × 1 surface. The success of this analogy advances the concept that the reactivity of a covalent surface can be well described within a molecular framework, and lends support to the notion of using known organic reactions to predict interfacial reactions of semiconductors. It therefore has been of great interest to test the generality of the surface cycloaddition reaction, and consequently we have performed studies to address whether cycloaddition reactions also occur on the surfaces of related covalent materials. The closest homologues to silicon for comparison are carbon and germanium, also in Group IV of the periodic table.

Both carbon (in its diamond form) and germanium are of technological interest. Silicon germanium alloys, for example, are used for high-frequency devices in applications such as wireless communications.^{108,109} Diamond has received much attention for its unique combination of material properties, such as high thermal conductivity, wide optical transparency, hardness, and chemical inertness.¹¹⁰ Like Si(100), the (100) crystallographic face of both Ge^{7,8} and diamond^{9,10} undergoes a (2 × 1) reconstruction to form rows of surface dimers. These dimers each are believed to have some degree of double-bond character, with a strong σ bond and a partial π bond.^{3,111} However, the surfaces differ in the strength of the π bond and the degree of tilt that is observed in the dimers. The dimers are symmetric on the C(100)-2 × 1 surface with the strongest π bond, buckled at low temperatures on Si(100)-2 × 1, and statically buckled even at room temperature on Ge(100)-2 × 1.^{5,6,9,10,28–31,111} On Si(100)-2 × 1, the dimers appear symmetric at room temperature by scanning tunneling microscopy due to rapid dynamic change in the direction of the tilt, except at certain defect sites.

Despite the differences in the dimer structure noted above, our studies have shown that the Diels–Alder product is formed on the (100)-2 × 1 surface of all three of these Group IV materials. The IR spectra of 1,3-butadiene chemisorbed on C(100)-2 × 1, Si(100)-2 × 1 and Ge(100)-2 × 1, together with the multilayer spectrum, are shown in Figure 6. On Ge(100)-2 × 1, the adsorption product shows close similarities in bonding with the Si(100)-2 × 1 product,¹¹² based upon the well-matched spectral features between the two surfaces. As in the case of Si(100)-2 × 1, the product on Ge(100)-2 × 1 can be assigned to the Diels–Alder adduct largely due to the absence of the high wavenumber (near 3080 cm⁻¹) terminal vinylic CH₂ stretch, since this functional group in the molecule would be lost upon formation of the Diels–Alder ring.

The reaction between butadiene and the C(100)-2 × 1 surface was also found to form predominantly the Diels–Alder product. This result is significant because unlike germanium or silicon, the diamond surface allows *direct comparison* to be made between carbon chemistry in a molecular system (i.e., organic chemistry) versus carbon chemistry on the surface of an extended solid (i.e., surface chemistry). The infrared spectrum of the C(100)-2 × 1 surface after exposure to 1,3-butadiene at room temperature is shown in Figure 6. To assign the chemisorbed product on C(100)-2 × 1, an isotopic substitution experiment using 1,3-butadiene-(1,1,4,4)-d₄

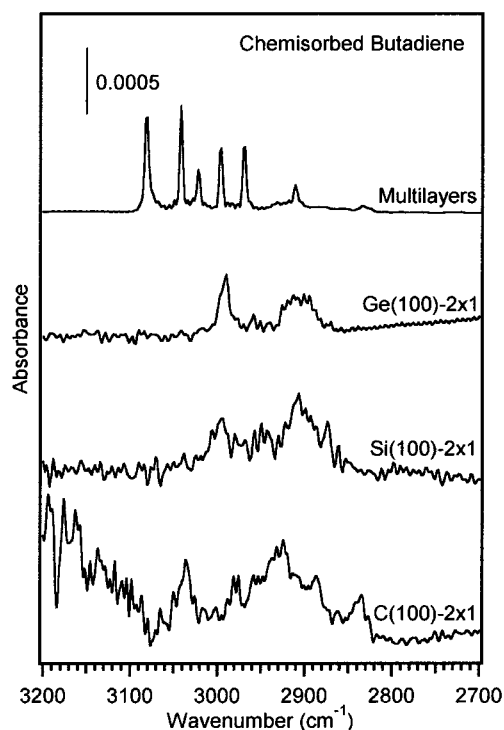


Figure 6. Infrared spectra of 1,3-butadiene chemisorbed on C(100)-2 × 1, Si(100)-2 × 1, and Ge(100)-2 × 1 surfaces. The 1,3-butadiene multilayer spectrum is shown for comparison. [Adapted from refs 112 and 120.]

(CD₂=CH–CH=CD₂) was also performed. The only feature remaining in the deuterated spectrum was found to be the highest energy mode at 3035 cm⁻¹, revealing that this mode stems from the internal carbons in the molecule, a result which is inconsistent with the [2+2] product. This analysis leads to the conclusion that butadiene forms predominantly the [4+2] product on C(100)-2 × 1.¹¹³ In addition, two small bumps were observed in the isotopomer spectrum at around 2930 and 2950 cm⁻¹; these peaks may signal the presence of secondary product at the surface. One possibility is a minor [2+2] side product. Recent theoretical calculations by Fitzgerald and Doren have investigated the butadiene/diamond(100) reaction system, and their results are consistent with the formation of a majority [4+2] product with a minor [2+2] product.¹⁰⁰

A comparison of the infrared spectra of butadiene chemisorbed on C(100)-2 × 1, Si(100)-2 × 1, and Ge(100)-2 × 1 (Figure 6) reveals that although the shapes of the spectra are similar, the peak positions on C(100) are shifted up relative to the other two surfaces. We have hypothesized that this shift is related to differences in ring strain in the adduct resulting from the greater length of the Si or Ge dimer bonds (~2.2–2.4 Å)^{5,6,28–31} compared to the C dimer (~1.4 Å)^{6,9,10,111} or to electron donation effects from the surface of Si versus C. A further difference between diamond and the Si or Ge surfaces is that significantly higher exposures of butadiene (~1–2 orders of magnitude) are required on C(100) than either Si(100) or Ge(100) to obtain saturation, indicating that the reaction is much less facile on the diamond surface. The lower reactivity of the C(100) surface with butadiene is likely the consequence of a stronger π bond: ca. 10–28 kcal/mol^{9,10,111} compared to 5–10 kcal/mol on Si(100).^{28–31} We note, however, that the C(100) studies were done in a different vacuum system than the Si and Ge studies, precluding precise quantification of the relative reactivities.

The thermal chemistry also differs between the surfaces. In contrast to Si, the Diels–Alder reaction is found to be reversible on Ge(100)-2 \times 1, leading to loss (by desorption) of the organic layer upon heating the surface to 570 K.¹¹² The reverse of the Diels–Alder reaction is called the retro-Diels–Alder reaction, and it also finds close parallels in molecular organic chemistry. The facility by which butadiene desorbs rather than decomposes on Ge(100)-2 \times 1 arises from the weaker strength of Ge–C versus Si–C bonds. Each Ge–C bond is nearly 10 kcal/mol weaker than a Si–C bond,⁶⁷ and upon thermal activation, desorption (cleavage of Ge–C bonds) can compete effectively with decomposition via C–H or C–C bond cleavage. In general, organics form weaker bonds to germanium than to silicon, and we expect that in many cases, more facile desorption or even shifting of competing product channels will be observed on the Ge surface as a result. On the other hand, the Diels–Alder adduct on diamond appears to decompose upon heating, consistent with stronger C–C bonds.¹¹⁴

Over the past few years, researchers have continued to probe for detailed parallels between the surface chemistry of Si(100) with that of Ge(100) and C(100). Adsorption studies of other olefinic molecules such as cyclohexadiene,¹¹⁵ cyclopentene,^{116–118} and ethylene¹¹ at the Ge(100)-2 \times 1 surface in ultrahigh vacuum have supported the conclusion that like Si, Ge(100) can participate in cycloaddition chemistry. Both [2+2] and [4+2] reaction products have been observed experimentally. Theoretical investigations have also revealed close parallels in energetics between cycloaddition reactions on Si(100) vs Ge(100). Namely, on both surfaces, the [4+2] cycloaddition product is more stable by approximately 15–20 kcal/mol than the [2+2] cycloaddition product.⁶⁷

On diamond, [2+2] reactions have also been observed in addition to [4+2] cycloaddition.^{100,119–122} Taken together, these studies have shown that the carbon dimers on the diamond(100) surface behave like C=C double bonds toward organic cycloaddition reactions. Recall that [2+2] cycloadditions are not generally observed in molecular systems because they are symmetry forbidden according to the Woodward–Hoffmann rules. At the surfaces of Si and Ge solids, [2+2] reactions are believed to occur because the tilted surface dimers and weak π bond provide an asymmetric reaction approach (three-member transition state) that reduces the barrier.^{51,60,104} It is reported that on diamond, the dimers do not tilt.^{5,6,9} Furthermore, the π bond of the diamond dimer is stronger than that of silicon or germanium.^{9,10,111} Of all the Group IV surface dimers, then, those of diamond would be expected to be most like their C=C analogue. Consistent with this expectation, it was found in a study by Hovis et al. that while cyclopentene does undergo [2+2] addition on C(100), the reaction probability is 3 orders of magnitude lower than that on Si(100) or Ge(100).^{117,121} The [4+2] reaction probability is also lower on C(100) relative to Si, but the effect is not as large. Both of these observations are consistent with the calculations by Fitzgerald and Doren showing that the barriers for these cycloaddition reactions are higher than those on silicon.¹⁰⁰

IV. Functionalization Using Amines

Unsaturated hydrocarbons make up just one class of molecules that can be used for attachment to semiconductor surfaces. Other functional groups, such as alcohols,^{123,124} amines,^{88,89,125–132} and carbonyls,^{133–136} may also undergo reaction to form strong bonds to the bare surface, and the success of the cycloaddition analysis suggests that parallels may be also found between these other attachment reactions and related organic chemistry. In this

section, we consider the reactivity of amine groups with the semiconductor surface. Amine chemistry at the Si(100)-2 \times 1 surface provides an excellent opportunity to explore in greater depth the reactivity of the surface dimers toward organic reagents.

In contrast to the description of the dimer used to treat cycloaddition chemistry, in which analogies were made to a double bond, it is most instructive to treat the surface dimer as a zwitterionic-type diradical in order to understand amine chemistry. As discussed previously, the most stable dimer configuration on the Si(100)-2 \times 1 surface is buckled (Figure 2). This buckling of the dimers results in a charge separation between the two dimer atoms. The down atom of the tilted dimer has a slightly positive charge relative to the up atom, introducing some zwitterionic characteristics into the weak π -bond of the dimer.¹³⁷ In other words, one atom in the dimer (the electron-rich up atom) is nucleophilic, and the other (the electron-poor down atom) is electrophilic. This molecular description provides for a successful interpretation of amine chemistry.

We have undertaken studies of the reactions of a series of model aliphatic amines (methylamine, dimethylamine, and trimethylamine) and their cyclic counterparts (pyrrolidine, methylpyrrolidine) with the Si surfaces. For this series, two principal reaction pathways were observed: dissociative adsorption via N–H bond cleavage, and molecular adsorption through a dative bond involving the nitrogen lone pair. The strongest factor influencing the reaction pathways of the molecules is found to be whether the molecules are primary, secondary, or tertiary amines. Within these classes, similar reactivity was seen for noncyclic versus cyclic amines.

A. N–C vs N–H Bond Cleavage on Silicon. Our experimental and theoretical studies both provide evidence that in dissociative adsorption of the alkylamines, N–H bond cleavage is favored over N–C bond cleavage. The N–H dissociation pathway is demonstrated clearly by infrared studies. Infrared spectra over the N–H, C–H, and Si–H stretching regions are shown in Figure 7 for pyrrolidine, dimethylamine, methylpyrrolidine, and trimethylamine after saturation exposures on Si(100)-2 \times 1 at room temperature (spectra on left) and in multilayers at low temperature (spectra on right). In Figure 7a,b, the spectra of the two secondary amines, pyrrolidine and dimethylamine, can be compared to their multilayer spectra, shown in Figure 7e,f. The N–H stretching modes near 3190 cm^{-1} present for both of these molecules in their physisorbed state have completely disappeared upon adsorption onto the Si(100)-2 \times 1 surface at room temperature. The loss of the N–H stretching mode together with the growth of an Si–H mode at 2070 cm^{-1} indicates that both pyrrolidine and dimethylamine dissociatively adsorb onto the Si(100)-2 \times 1 surface via N–H bond cleavage. The reaction leaves the molecule covalently attached to the surface by a N–Si bond, with the remaining H atom bonded to a Si atom.^{130,131}

The observation of N–H bond cleavage in amines is consistent with previous studies of amines on clean Si(100)-2 \times 1.^{88,89,125–131} Furthermore, both experimental and theoretical studies have shown that ammonia reacts by scission of an N–H bond to produce surface $\text{NH}_2(\text{a})$ and $\text{H}(\text{a})$ species.^{137–152} The reaction of aniline was found to occur via N–H dissociation similar to ammonia, resulting in nonbridge bonded surface species.^{125,127} 3-pyrroline was shown to adsorb onto the Si(100)-2 \times 1 surface via two competing pathways, namely [2+2] cycloaddition and N–H dissociation.^{88,89,129} Other nitrogen-containing reagents were also studied using several

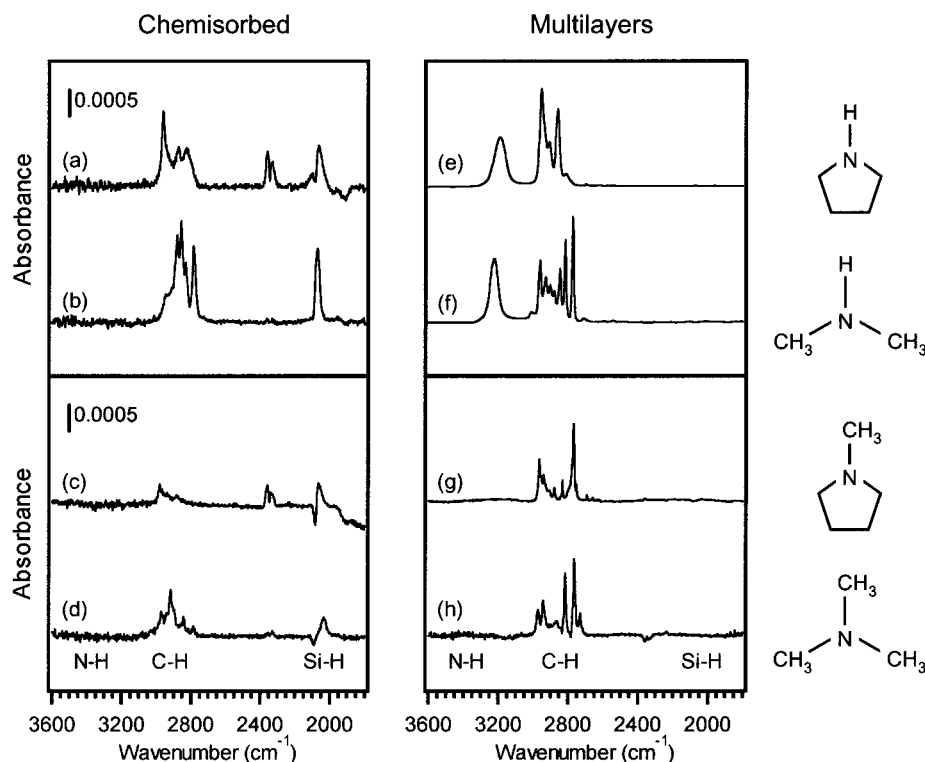


Figure 7. Infrared spectra of secondary and tertiary amines at the Si(100)-2 \times 1 surface. Spectra of chemisorbed (a) pyrrolidine, (b) dimethylamine, (c) methylpyrrolidine, and (d) trimethylamine were obtained for saturation coverages at 300 K. Spectra of multilayers of (e) pyrrolidine, (f) dimethylamine, (g) methylpyrrolidine, and (h) trimethylamine were collected at 100–115 K. [Adapted from refs 130 and 131.]

experimental techniques, including 1,1-dimethylhydrazine,¹⁵³ dimethylamine,¹⁵⁴ and pyrrole.^{128,129}

The experimentally observed favoring of N–H bond cleavage over N–C bond scission is elucidated by the results of our theoretical calculations. Here we use dimethylamine as an example to illustrate the theoretical approach and interpretation.¹³⁰ Figure 8 shows energetics for both the N–H and N–CH₃ bond dissociation pathways for dimethylamine calculated at a Si₉H₁₂ one-dimer silicon cluster. Initial adsorption of dimethylamine results in a stable, molecularly adsorbed state with an adsorption energy of nearly 25 kcal/mol. As discussed below, the molecularly adsorbed precursor state involves a dative bond between the nitrogen lone-pair and the electrophilic down-atom of the buckled Si dimer.^{24,137,147} From the dative-bonded state, calculations show the barrier for dimethylamine to proceed to cleave the N–H bond is located below the vacuum level, and the formation of surface N(CH₃)₂(a) and H(a) species is exothermic by over 50 kcal/mol. In contrast, although the pathway for N–C bond cleavage is more exothermic (<–65 kcal/mol) than that for N–H bond cleavage, the barrier for N–CH₃ dissociation is 19.3 kcal/mol above the vacuum level. Hence, this process is activated, and N–C bond cleavage would not be expected to occur at room temperature.

To understand why the activation energies differ between the two pathways and to gain additional insight into the process, we will examine the transition state geometries.¹³⁰ Figure 9 shows the highest occupied molecular orbitals (HOMO's) of the transition states for N–H and N–CH₃ dissociation of dimethylamine on the one-dimer cluster. As electron density is donated from the amine lone pair to the down silicon atom upon adsorption into the precursor state, the up Si atom in the dimer becomes electron rich, as shown in Figure 9. At this stage, the dative bonded precursor can be described as a quaternary ammonium ion. The N–H dissociation pathway can thus be interpreted as the transfer of a proton from the ammonium ion

to the electron rich up Si atom through a Lewis acid–base reaction. The highest occupied molecular orbital (HOMO) of the N–H cleavage transition state shows that electron density from the Lewis-basic up Si atom interacts with the N–H σ -bond from the backside of the H atom. In the transition state, the N–H and Si–H bond lengths are only 21% longer and 29% longer than those in the molecularly adsorbed state and the H dissociation state, respectively, leading to a relatively low activation barrier.

In contrast, the N–CH₃ dissociation pathway is best described as a nucleophilic substitution reaction, where the electron rich up Si atom of the dimer acts as a nucleophile, and the amine molecule attached to the down Si atom is the leaving group. Inspection of the transition state HOMO shows that the nucleophilic Si atom attacks the methyl group from its *front* side, where the leaving amine group is bonded. Backside attack of the methyl group by the up Si atom is energetically unfavorable due to steric hindrance of the methyl hydrogens. Consequently, the N–C bond has to be stretched in order to accommodate front side nucleophilic attack. The N–C and the Si–C bond lengths in this transition state are stretched 36% and 63%, respectively, relative to the corresponding N–C and Si–C bonds in the reactant and the product. As a result, the energy of the transition state is raised and hence the N–CH₃ dissociation process has a relatively high activation barrier.¹³⁰ The results are also consistent with organonitrogen chemistry, where for quaternary ammonium ions, abstraction of a proton from tetravalent nitrogen by a base (in this case the electron-rich “up” Si atom) is typically kinetically easy compared to N–C cleavage.¹⁵⁵

The results indicate that the selectivity of N–H cleavage over N–CH₃ dissociation for amines on the Si(100)-2 \times 1 surface is kinetically controlled, and not the result of thermodynamic control. Although the calculation is shown here only for dimethylamine, similar computational analysis shows that the

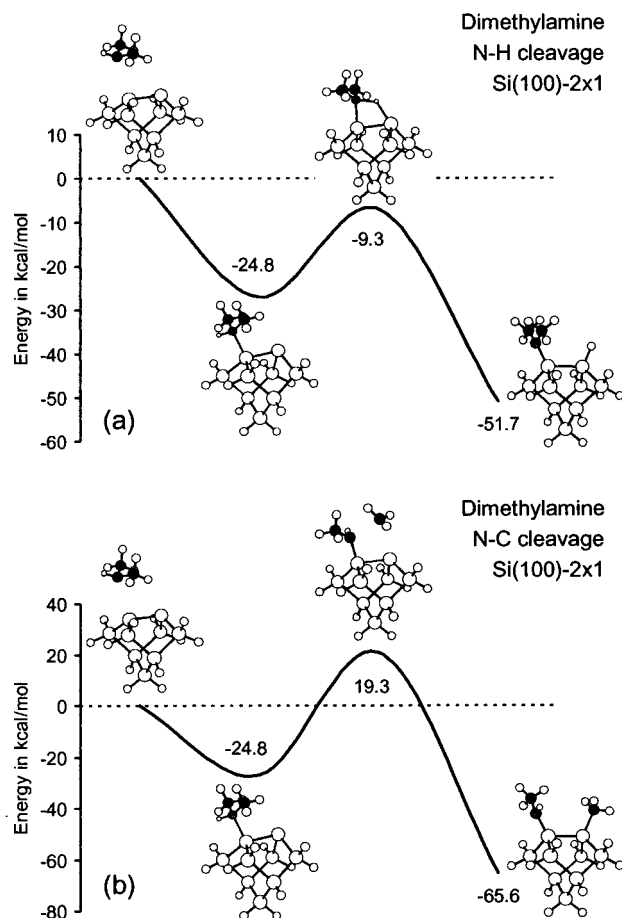


Figure 8. Calculated reaction path and optimized structures for (a) N–H dissociation and (b) N–CH₃ dissociation of dimethylamine on the Si one-dimer cluster. [Adapted from ref 130.]

kinetic selectivity holds for other amines such as methylamine and pyrrolidine on Si.^{130,131}

B. Dative Bonds. As shown in the previous analysis, N–CH₃ dissociation is kinetically inaccessible at room temperature. Therefore, molecules without N–H bonds, such as tertiary aliphatic amines (e.g., trimethylamine and methylpyrrolidine), will become trapped in the molecular precursor state at the Si(100)-2 × 1 surface, shown in Figure 8 for dimethylamine. The precursor state is one in which the nitrogen lone pair forms a dative bond to the electrophilic (down) atom of the Si dimer. This interaction is essentially a Lewis acid–base reaction, where the amine is the Lewis base and the silicon the Lewis acid. The stability of this precursor state can be shown using a simple first-order kinetic analysis. Held by a barrier of greater than 25 kcal/mol for either dissociation or molecular desorption, the molecularly adsorbed amine will exhibit a residence time at room temperature of $t_{1/2} \sim 3500$ h. Hence, according to theoretical calculations and kinetics arguments, trimethylamine and methylpyrrolidine will trap into the dative-bonded state at room temperature.

The corresponding infrared spectra present clear experimental evidence for the formation of a dative bond at the surface. Parts c and d of Figure 7 show infrared spectra of methylpyrrolidine and trimethylamine following a saturation dose on Si(100)-2 × 1 at room temperature, and parts g and h of Figure 7 show spectra of multilayers of these molecules at low temperature. For both of these tertiary amines, the absorption spectra in the C–H stretching region are similar to their multilayer spectra, with the notable exception that the peaks

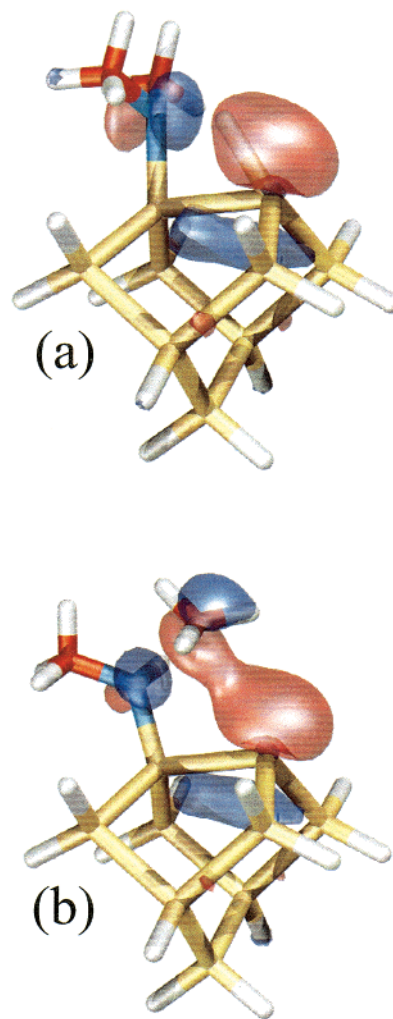


Figure 9. Orbital interpretation of the N–H and N–C dissociation transition states for dimethylamine, showing the highest occupied molecular orbitals (HOMO). [Adapted from ref 130.]

below 2800 cm⁻¹ have disappeared upon adsorption to the silicon surface. Such extraordinarily low C–H stretching frequencies are known as Bohlmann bands. They originate from the interaction of the nitrogen lone pair orbital with the C–H σ orbitals trans periplanar to the lone pair, causing an increase in bond lengths, a decrease in bond energies and hence a downshift in vibrational frequencies. The downshift in frequencies caused by the *trans*-lone-pair effect and the effect of methyl substitution on the frequencies of the Bohlmann bands have been studied in detail by infrared spectroscopy of deuterium substituted amines.¹⁵⁶ The loss of these *trans*-lone-pair modes upon adsorption indicates that both methylpyrrolidine and trimethylamine are molecularly bonded to Si at room temperature through the nitrogen lone pair, which is no longer available to perturb the *trans* C–H bonds.¹³¹

It can be seen from Figure 7 that the tertiary amines adsorbed through the dative bond produce a weaker infrared spectrum than the secondary amines that bond via N–H cleavage. For example, the integrated intensities of the $\nu(\text{C–H})$ stretching modes of adsorbed pyrrolidine is 6 times that of methylpyrrolidine. While the use of IR intensities to quantitatively compare relative coverages of two different surface species can be unreliable, it does provide a means to make a qualitative comparison. If we assume that the cross sections for the IR modes of the different molecules are similar, then we can conclude that the coverage of the dative-bonded tertiary amines

is several times lower than that of the dissociatively adsorbed secondary amines at saturation. This observation has been attributed to both steric and electronic effects that differ between the dative bond and the dissociative state at the surface.^{130,131}

V. Concluding Remarks

The surfaces of the Group IV semiconductors — Si(100)-2 × 1, Ge(100)-2 × 1, and C(100)-2 × 1 — provide a solid template upon which an organic layer can be attached by means of a variety of different reactions. Here we reviewed our investigations into two classes of organic attachment reactions that maintain strong parallels with molecular systems. We have shown that Diels–Alder products can be formed in the reaction of conjugated dienes with the dimers of the Si(100)-2 × 1, Ge(100)-2 × 1, and C(100)-2 × 1 surfaces. This is one example out of a group of cycloaddition reactions that have been shown to occur at these surfaces, leading to the formation of strong covalent linkages between organic molecules and the surface. We have also investigated amine functionalities, which demonstrate a preference for attaching at the Si surface via N–H rather than N–C cleavage, in accordance with organic analogues. Furthermore, we have shown using both experiment and theory that tertiary amines form dative bonds to the surface through an interaction between the lone pair of the amine molecule and the electron-deficient down atom of the Si dimer.

Conceptually, the framework for describing certain reactions in organic chemistry appears to apply similarly to the surface reactions. These parallels allow one to apply the broad knowledge base available from organic chemistry to tailor the reactions at the surface in order to obtain targeted products. These, and other, classes of reactions may lead to further understanding of chemical properties of semiconductor interfaces and to the development of new techniques of semiconductor surface functionalization.

Organic functionalization of semiconductors is an emerging area in interface science. This technology provides the opportunity to create hybrid devices exploiting the properties and features of both organic and inorganic materials. At a molecular level, by proper choice of organic reagent one can potentially engineer a variety of useful surface layers, including layers exhibiting chirality, molecular recognition, conductivity, or nonlinear optical properties. The properties engineered into the organic layers at the interface may lead to the enabling of numerous applications, including lubrication, optical response, chemical sensing, or the extension of biocompatibility to semiconductor surfaces.

A number of challenges remain, however, before many of these presumed applications—in nanotechnology, sensing, and others areas—can be realized using this technology. One future need is to increase the degree of control over both the selectivity toward one product over another, and the degree of order in the organic layer. This in turn requires a deeper understanding of the driving forces that control the attachment reactions. Evidence presented in this article points to the importance of kinetic control over thermodynamics in these reaction systems. However, recent examples have been found of thermodynamically controlled reactions on semiconductors, as well.¹³⁶ Therefore, it is important to understand how to design the system (by choice of reaction conditions or molecular precursors) to control and manipulate the product distribution. More work is also needed in determining the detailed reaction mechanisms.

One of the key challenges is the ability to deposit multiple organic layers in a controllable fashion. So far, most of the work in organic functionalization by covalent Si–C attachment has

focused on the initial monolayer. A nice exception is the work by Bitzer and Richardson.^{157,158} It is clear that many applications require flexibility in the deposition of multiple layers. To extend the organic modification to allow for next-layer attachment, a bifunctional or polyfunctional organic molecule must be used for the first layer. This layer, in turn, will need to retain a reactive functional group for further attachment. One approach is to use symmetric bifunctional compounds, so that competition between different functional groups is avoided. Rigidity may be necessary in such molecules to prevent both ends from attaching to the surface. Another approach is to utilize protecting group strategies common in organic synthesis: to block off reaction at the protected functional group until later deprotection and reaction. There is clearly a great need not only for understanding how different functional groups react at the semiconductor surface, but also for learning how to utilize different means of directing the reaction of a polyfunctional molecule in a controlled fashion.

There are a number of exciting opportunities in the area of organic functionalization of semiconductors. The ability to covalently attach organic layers to the surfaces of semiconducting solids is an emerging area with links to a variety of new technologies. The successful implementation of organic attachment to semiconductors is expected to impact a number of developing fields.

Acknowledgment. The author expresses appreciation to the many students and colleagues who contributed immensely to the work described in this review, including A. V. Teplyakov, M. Kong Moreno, G. T. Wang, C. Mui, C. B. Musgrave, D. J. Doren, and J. N. Russell. Special thanks are due to Collin Mui for a careful reading of the manuscript and for contributions to the figures. The work was supported by the National Science Foundation (under Grants DMR-9896333 and CHE-9900041) and the Beckman Foundation. The author also thanks the Camille and Henry Dreyfus Foundation for support through a Teacher-Scholar award.

References and Notes

- Hamers, R. J.; Tromp, R. M.; Demuth, J. E. *Phys. Rev. B* **1986**, *34*, 5343.
- Boland, J. J. *Adv. Phys.* **1993**, *42*, 129.
- Duke, C. B. *Chem. Rev.* **1996**, *96*, 1237.
- Kubby, J. A.; Boland, J. J. *Surf. Sci. Rep.* **1996**, *26*, 61.
- Kruger, P.; Pollmann, J. *Phys. Rev. Lett.* **1995**, *74*, 1155.
- Yang, C.; Kang, H. C. *J. Chem. Phys.* **1999**, *110*, 11029.
- Kubby, J. A.; Griffith, J. E.; Becker, R. S.; Vickers, J. S. *Phys. Rev. B* **1987**, *36*, 6079.
- Torrelles, X.; vanderVegt, H. A.; Etgens, V. H.; Fajardo, P.; Alvarez, J.; Ferrer, S. *Surf. Sci.* **1996**, *364*, 242.
- Thoms, B. D.; Butler, J. E. *Surf. Sci.* **1995**, *328*, 291.
- Mercer, T. W.; Pehrsson, P. E. *Surf. Sci.* **1998**, *399*, L327.
- Lal, P.; Teplyakov, A. V.; Noah, Y.; Kong, M. J.; Wang, G. T.; Bent, S. F. *J. Chem. Phys.* **1999**, *110*, 10545.
- Kong, M. J.; Lee, K. S.; Lyubovitsky, J.; Bent, S. F. *Chem. Phys. Lett.* **1996**, *263*, 1.
- Kim, C. S.; Mowrey, R. C.; Butler, J. E.; Russell, J. N. *J. Phys. Chem. B* **1998**, *102*, 9290.
- Chabal, Y. J.; Raghavachari, K. *Phys. Rev. Lett.* **1984**, *53*, 282.
- Crowell, J. E.; Lu, G. Q. *J. Electron Spectrosc. Relat. Phenom.* **1990**, *54*, 1045.
- Thoms, B. D.; Owens, M. S.; Butler, J. E.; Spiro, C. *Appl. Phys. Lett.* **1994**, *65*, 2957.
- Mercer, T. W.; Russell, J. N.; Pehrsson, P. E. *Surf. Sci.* **1997**, *392*, L21.
- Fischer, D. A.; Colbert, J.; Gland, J. L. *Rev. Sci. Instrum.* **1989**, *60*, 1596.
- Outka, D. A.; Stohr, J. *J. Chem. Phys.* **1988**, *88*, 3539.
- Kohn, W.; Sham, L. J. *Phys. Rev.* **1965**, *140*, A1133.
- Hohenberg, P.; Kohn, W. *Phys. Rev.* **1964**, *136*, B864.

- (22) Frisch, M. J.; Trucks, G. W.; Schlegel, H. B.; Scuseria, G. E.; Robb, M. A.; Cheeseman, J. R.; Zakrzewski, V. G.; Montgomery, J. A. J.; Stratmann, R. E.; Burant, J. C.; Dapprich, S.; Millam, J. M.; Daniels, A. D.; Kudin, K. N.; Strain, M. C.; Farkas, O.; Tomasi, J.; Barone, V.; Cossi, M.; Cammi, R.; Mennucci, B.; Pomelli, C.; Adamo, C.; Clifford, S.; Ochterski, J.; Petersson, G. A.; Ayala, P. Y.; Cui, Q.; Morokuma, K.; Malick, D. K.; Rabuck, A. D.; Raghavachari, K.; Foresman, J. B.; Cioslowski, J.; Ortiz, J. V.; Stefanov, B. B.; Liu, G.; Liashenko, A.; Piskorz, P.; Komaromi, I.; Gomperts, R.; Martin, R. L.; Fox, D. J.; Keith, T.; Al-Laham, M. A.; Peng, C. Y.; Nanayakkara, A.; Gonzalez, C.; Challacombe, M.; Gill, P. M. W.; Johnson, B.; Chen, W.; Wong, M. W.; Andres, J. L.; Gonzalez, C.; Head-Gordon, M.; Replogle, E. S.; Pople, J. A. *Gaussian 98*; revision A.5; Gaussian, Inc.: Pittsburgh, PA, 1998.
- (23) Konecny, R.; Doren, D. J. *Surf. Sci.* **1998**, *417*, 169.
- (24) Widjaja, Y.; Musgrave, C. B. *Surf. Sci.* **2000**, *469*, 9.
- (25) Becke, A. D. *Phys. Rev. A* **1988**, *38*, 3098.
- (26) Lee, C. T.; Yang, W. T.; Parr, R. G. *Phys. Rev. B* **1988**, *37*, 785.
- (27) Becke, A. D. *J. Chem. Phys.* **1993**, *98*, 5648.
- (28) Wu, C. J.; Carter, E. A. *Chem. Phys. Lett.* **1991**, *185*, 172.
- (29) Nachtigall, P.; Jordan, K. D.; Sosa, C. J. *Phys. Chem.* **1993**, *97*, 11666.
- (30) D' Evelyn, M. P.; Yang, Y. M. L.; Sutcu, L. F. *J. Chem. Phys.* **1992**, *96*, 852.
- (31) Hofer, U.; Li, L. P.; Heinz, T. F. *Phys. Rev. B* **1992**, *45*, 9485.
- (32) Wassermann, A. *Diels-Alder Reactions: Organic Background and Physico-Chemical Aspects*; Elsevier: New York, 1965.
- (33) Carruthers, W. *Cycloaddition Reactions in Organic Synthesis*; Pergamon Press: New York, 1990.
- (34) Fallis, A. G. *Acc. Chem. Res.* **1999**, *32*, 464.
- (35) Woodward, R. B.; Hoffmann, R. *The Conservation of Orbital Symmetry*; Academic Press: New York, 1970.
- (36) Bozack, M. J.; Choyke, W. J.; Muehlhoff, L.; Yates, J. T. *J. Appl. Phys.* **1986**, *60*, 3750.
- (37) Nishijima, M.; Yoshinobu, J.; Tsuda, H.; Onchi, M. *Surf. Sci.* **1987**, *192*, 383.
- (38) Yoshinobu, J.; Tsuda, H.; Onchi, M.; Nishijima, M. *J. Chem. Phys.* **1987**, *87*, 7332.
- (39) Cheng, C. C.; Choyke, W. J.; Yates, J. T. *Surf. Sci.* **1990**, *231*, 289.
- (40) Clemen, L.; Wallace, R. M.; Taylor, P. A.; Dresser, M. J.; Choyke, W. J.; Weinberg, W. H.; Yates, J. T. *Surf. Sci.* **1992**, *268*, 205.
- (41) Taylor, P. A.; Wallace, R. M.; Cheng, C. C.; Weinberg, W. H.; Dresser, M. J.; Choyke, W. J.; Yates, J. T. *J. Am. Chem. Soc.* **1992**, *114*, 6754.
- (42) Huang, C.; Widdra, W.; Wang, X. S.; Weinberg, W. H. *J. Vac. Sci. Technol. A* **1993**, *11*, 2250.
- (43) Mayne, A. J.; Avery, A. R.; Knall, J.; Jones, T. S.; Briggs, G. A. D.; Weinberg, W. H. *Surf. Sci.* **1993**, *284*, 247.
- (44) Huang, C.; Widdra, W.; Weinberg, W. H. *Surf. Sci.* **1994**, *315*, L953.
- (45) Widdra, W.; Huang, C.; Briggs, G. A. D.; Weinberg, W. H. *J. Electron Spectrosc. Relat. Phenom.* **1993**, *64-5*, 129.
- (46) Chua, L. H.; Jackman, R. B.; Foord, J. S. *Surf. Sci.* **1994**, *315*, 69.
- (47) Chen, Y.; Liu, Z. H.; Zhang, Q. Z.; Feng, K.; Lin, Z. D. *Appl. Phys. Lett.* **1995**, *67*, 2936.
- (48) Liu, Q.; Hoffmann, R. J. *Am. Chem. Soc.* **1995**, *117*, 4082.
- (49) Fisher, A. J.; Blochl, P. E.; Briggs, G. A. D. *Surf. Sci.* **1997**, *374*, 298.
- (50) Meng, B. Q.; Maroudas, D.; Weinberg, W. H. *Chem. Phys. Lett.* **1997**, *278*, 97.
- (51) Liu, H. B.; Hamers, R. J. *J. Am. Chem. Soc.* **1997**, *119*, 7593.
- (52) Pan, W.; Zhu, T. H.; Yang, W. T. *J. Chem. Phys.* **1997**, *107*, 3981.
- (53) Tindall, C.; Li, L.; Takaoka, O.; Hasegawa, Y.; Sakurai, T. *J. Korean Phys. Soc.* **1997**, *31*, S23.
- (54) Birkenheuer, U.; Gutdeutsch, U.; Rosch, N.; Fink, A.; Gokhale, S.; Menzel, D.; Trischberger, P.; Widdra, W. *J. Chem. Phys.* **1998**, *108*, 9868.
- (55) Matsui, F.; Yeom, H. W.; Imanishi, A.; Isawa, K.; Matsuda, I.; Ohta, T. *Surf. Sci.* **1998**, *401*, L413.
- (56) Casaletto, M. P.; Zanon, R.; Carbone, M.; Piancastelli, M. N.; Aballe, L.; Weiss, K.; Horn, K. *Phys. Rev. B* **2000**, *62*, 17128.
- (57) Lu, X.; Lin, M. C. *Phys. Chem. Chem. Phys.* **2000**, *2*, 4213.
- (58) Matsui, F.; Yeom, H. W.; Matsuda, I.; Ohta, T. *Phys. Rev. B* **2000**, *62*, 5036.
- (59) Tanida, Y.; Tsukada, M. *Appl. Surf. Sci.* **2000**, *159*, 19.
- (60) Lopinski, G. P.; Moffatt, D. J.; Wayner, D. D. M.; Wolkow, R. A. *J. Am. Chem. Soc.* **2000**, *122*, 3548.
- (61) Terborg, R.; Baumgartel, P.; Lindsay, R.; Schaff, O.; Giessel, T.; Hoeft, J. T.; Polcik, M.; Toomes, R. L.; Kulkarni, S.; Bradshaw, A. M.; Woodruff, D. P. *Phys. Rev. B* **2000**, *61*, 16697.
- (62) Xu, S. H.; Keffe, M.; Yang, Y.; Chen, C.; Yu, M.; Lapeyre, G. J.; Rotenberg, E.; Denlinger, J.; Yates, J. T. *Phys. Rev. Lett.* **2000**, *84*, 939.
- (63) Cho, J. H.; Kleinman, L.; Chan, C. T.; Kim, K. S. *Phys. Rev. B* **2001**, *6307*, 3306.
- (64) Morikawa, Y. *Phys. Rev. B* **2001**, *6303*, 3405.
- (65) Wolkow, R. A. *Annu. Rev. Phys. Chem.* **1999**, *50*, 413.
- (66) Choi, C. H.; Gordon, M. S. *J. Am. Chem. Soc.* **1999**, *121*, 11311.
- (67) Mui, C.; Bent, S. F.; Musgrave, C. B. *J. Phys. Chem. A* **2000**, *104*, 2457.
- (68) Taguchi, Y.; Fujisawa, M.; Takaoka, T.; Okada, T.; Nishijima, M. *J. Chem. Phys.* **1991**, *95*, 6870.
- (69) Craig, B. I. *Surf. Sci.* **1993**, *280*, L279.
- (70) Birkenheuer, U.; Gutdeutsch, U.; Rosch, N. *Surf. Sci.* **1998**, *409*, 213.
- (71) Borovsky, B.; Krueger, M.; Ganz, E. *Phys. Rev. B* **1998**, *57*, R4269.
- (72) Gokhale, S.; Trischberger, P.; Menzel, D.; Widdra, W.; Droge, H.; Steinruck, H. P.; Birkenheuer, U.; Gutdeutsch, U.; Rosch, N. *J. Chem. Phys.* **1998**, *108*, 5554.
- (73) Kong, M. J.; Teplyakov, A. V.; Lyubovitsky, J. G.; Bent, S. F. *Surf. Sci.* **1998**, *411*, 286.
- (74) Lopinski, G. P.; Fortier, T. M.; Moffatt, D. J.; Wolkow, R. A. *J. Vac. Sci. Technol. A* **1998**, *16*, 1037.
- (75) Lopinski, G. P.; Moffatt, D. J.; Wolkow, R. A. *Chem. Phys. Lett.* **1998**, *282*, 305.
- (76) Self, K. W.; Pelzel, R. I.; Owen, J. H. G.; Yan, C.; Widdra, W.; Weinberg, W. H. *J. Vac. Sci. Technol. A* **1998**, *16*, 1031.
- (77) Taguchi, Y.; Ohta, Y.; Katsumi, T.; Ichikawa, K.; Aita, O. *J. Electron Spectrosc. Relat. Phenom.* **1998**, *88*, 671.
- (78) Wolkow, R. A.; Lopinski, G. P.; Moffatt, D. J. *Surf. Sci.* **1998**, *416*, L1107.
- (79) Borovsky, B.; Krueger, M.; Ganz, E. *J. Vac. Sci. Technol. B* **1999**, *17*, 7.
- (80) Alavi, S.; Rousseau, R.; Lopinski, G. P.; Wolkow, R. A.; Seideman, T. *Faraday Discuss.* **2000**, 213.
- (81) Alavi, S.; Rousseau, R.; Seideman, T. *J. Chem. Phys.* **2000**, *113*, 4412.
- (82) Coulter, S. K.; Hovis, J. S.; Ellison, M. D.; Hamers, R. J. *J. Vac. Sci. Technol. A* **2000**, *18*, 1965.
- (83) Kong, M. J.; Teplyakov, A. V.; Jagmohan, J.; Lyubovitsky, J. G.; Mui, C.; Bent, S. F. *J. Phys. Chem. B* **2000**, *104*, 3000.
- (84) Schwartz, M. P.; Ellison, M. D.; Coulter, S. K.; Hovis, J. S.; Hamers, R. J. *J. Am. Chem. Soc.* **2000**, *122*, 8529.
- (85) Silvestrelli, P. L.; Ancilotto, F.; Toigo, F. *Phys. Rev. B* **2000**, *62*, 1596.
- (86) Stauffer, M.; Birkenheuer, U.; Belling, T.; Nortemann, F.; Rosch, N.; Widdra, W.; Kostov, K. L.; Moritz, T.; Menzel, D. *J. Chem. Phys.* **2000**, *112*, 2498.
- (87) Hofer, W. A.; Fisher, A. J.; Lopinski, G. P.; Wolkow, R. A. *Phys. Rev. B* **2001**, *6308*, 5314.
- (88) Hovis, J. S.; Lee, S.; Liu, H. B.; Hamers, R. J. *J. Vac. Sci. Technol. B* **1997**, *15*, 1153.
- (89) Liu, H. B.; Hamers, R. J. *Surf. Sci.* **1998**, *416*, 354.
- (90) Hovis, J. S.; Liu, H.; Hamers, R. J. *Appl. Phys. A* **1998**, *66*, S553.
- (91) Akiyama, R.; Matsumoto, T.; Kawai, T. *Phys. Rev. B* **2000**, *62*, 2034.
- (92) Yamashita, Y.; Nagao, M.; Machida, S.; Hamaguchi, K.; Yasui, F.; Mukai, K.; Yoshinobu, J. *J. Electron Spectrosc. Relat. Phenom.* **2001**, *114*, 389.
- (93) Yamashita, Y.; Hamaguchi, K.; Machida, S.; Mukai, K.; Yoshinobu, J.; Tanaka, S.; Kamada, M. *Appl. Surf. Sci.* **2001**, *169*, 172.
- (94) Yoshinobu, J.; Yamashita, Y.; Yasui, F.; Mukai, K.; Akagi, K.; Tsuneyuki, S.; Hamaguchi, K.; Machida, S.; Nagao, M.; Sato, T.; Iwatsuki, M. *J. Electron Spectrosc. Relat. Phenom.* **2001**, *114*, 383.
- (95) Hamaguchi, K.; Machida, S.; Mukai, K.; Yamashita, Y.; Yoshinobu, J. *Phys. Rev. B* **2000**, *62*, 7576.
- (96) Hovis, J. S.; Hamers, R. J. *J. Phys. Chem. B* **1997**, *101*, 9581.
- (97) Jolly, F.; Bournel, F.; Rochet, F.; Dufour, G.; Sirotti, F.; Taleb, A. *Phys. Rev. B* **1999**, *60*, 2930.
- (98) Bournel, F.; Jolly, F.; Rochet, F.; Dufour, G.; Sirotti, F.; Torelli, P. *Phys. Rev. B* **2000**, *62*, 7645.
- (99) Konecny, R.; Doren, D. J. *J. Am. Chem. Soc.* **1997**, *119*, 11098.
- (100) Fitzgerald, D. R.; Doren, D. J. *J. Am. Chem. Soc.* **2000**, *122*, 12334.
- (101) Teplyakov, A. V.; Kong, M. J.; Bent, S. F. *J. Chem. Phys.* **1998**, *108*, 4599.
- (102) Stöhr, J. *NEXAFS Spectroscopy*; Springer-Verlag: New York, 1992.
- (103) Mui, C.; Musgrave, C. B. Unpublished results.
- (104) Hovis, J. S.; Liu, H. B.; Hamers, R. J. *J. Phys. Chem. B* **1998**, *102*, 6873.
- (105) Doren, D. J. Private communication.
- (106) Hovis, J. S.; Liu, H.; Hamers, R. J. *Surf. Sci.* **1998**, *404*, 1.
- (107) Wang, G. T.; Mui, C.; Musgrave, C. B.; Bent, S. F. *J. Phys. Chem. B* **1999**, *103*, 6803.
- (108) Larson, L. E. *J. Vac. Sci. Technol. B* **1998**, *16*, 1541.
- (109) Meyerson, B. S. *IBM J. Res. Dev.* **2000**, *44*, 391.

- (110) Field, J. E., Ed. *The Properties of Natural and Synthetic Diamond*; Academic Press: London, 1992.
- (111) Hukka, T. I.; Pakkanen, T. A.; Develyn, M. P. *J. Phys. Chem.* **1994**, *98*, 12420.
- (112) Teplyakov, A. V.; Lal, P.; Noah, Y. A.; Bent, S. F. *J. Am. Chem. Soc.* **1998**, *120*, 7377.
- (113) It is important to note that dissociative chemisorption is deemed unlikely by the absence in the chemisorption spectrum of a sharp doublet at 2898 and 2919 cm^{-1} , which is characteristic of hydrogen on C(100).
- (114) Wang, G. T.; Bent, S. F.; Russell, J. N.; Butler, J. E.; D'Evelyn, M. P. Unpublished data.
- (115) Lee, S. W.; Nelen, L. N.; Ihm, H.; Scoggins, T.; Greenlief, C. M. *Surf. Sci.* **1998**, *410*, L773.
- (116) Lee, S. W.; Hovis, J. S.; Coulter, S. K.; Hamers, R. J.; Greenlief, C. M. *Surf. Sci.* **2000**, *462*, 6.
- (117) Hamers, R. J.; Coulter, S. K.; Ellison, M. D.; Hovis, J. S.; Padowitz, D. F.; Schwartz, M. P.; Greenlief, C. M.; Russell, J. N. *Acc. Chem. Res.* **2000**, *33*, 617.
- (118) Hamers, R. J.; Hovis, J. S.; Greenlief, C. M.; Padowitz, D. F. *Jpn. J. Appl. Phys., Part 1* **1999**, *38*, 3879.
- (119) Hossain, M. Z.; Aruga, T.; Takagi, N.; Tsuno, T.; Fujimori, N.; Ando, T.; Nishijima, M. *Jpn. J. Appl. Phys., Part 2* **1999**, *38*, L1496.
- (120) Wang, G. T.; Bent, S. F.; Russell, J. N.; Butler, J. E.; D'Evelyn, M. P. *J. Am. Chem. Soc.* **2000**, *122*, 744.
- (121) Hovis, J. S.; Coulter, S. K.; Hamers, R. J.; D'Evelyn, M. P.; Russell, J. N.; Butler, J. E. *J. Am. Chem. Soc.* **2000**, *122*, 732.
- (122) Russell, J. N., Jr.; Butler, J. E.; Wang, G. T.; Bent, S. F.; Hovis, J. S.; Hamers, R. J.; D'Evelyn, M. P. *Mater. Chem. Phys.* **2001**, *72*, 147.
- (123) Eng, J., Jr.; Raghavachari, K.; Struck, L. M.; Chabal, Y. J.; Bent, B. E.; Flynn, G. W.; Christman, S. B.; Chaban, E. E.; Williams, G. P.; Radermacher, K.; Mantl, S. *J. Chem. Phys.* **1997**, *106*, 9889.
- (124) Casaletto, M. P.; Zanon, R.; Carbone, M.; Piancastelli, M. N.; Aballe, L.; Weiss, K.; Horn, K. *Surf. Sci.* **2000**, *447*, 237.
- (125) Kugler, T.; Thibaut, U.; Abraham, M.; Folkers, G.; Gopel, W. *Surf. Sci.* **1992**, *260*, 64.
- (126) Bitzer, T.; Alkumshalie, T.; Richardson, N. V. *Surf. Sci.* **1996**, *368*, 202.
- (127) Rummel, R. M.; Ziegler, C. *Surf. Sci.* **1998**, *418*, 303.
- (128) Qiao, M. H.; Cao, Y.; Deng, J. F.; Xu, G. Q. *Chem. Phys. Lett.* **2000**, *325*, 508.
- (129) Cao, X.; Coulter, S. K.; Ellison, M. D.; Liu, H.; Liu, J.; Hamers, R. J. *J. Phys. Chem. B* **2001**, *105*, 3759.
- (130) Mui, C.; Wang, G. T.; Bent, S. F.; Musgrave, C. B. *J. Chem. Phys.* **2001**, *114*, 10170.
- (131) Wang, G. T.; Mui, C.; Musgrave, C. B.; Bent, S. F. *J. Phys. Chem. B* **2001**, *105*, 3295.
- (132) Cao, X.; Hamers, R. J. *J. Am. Chem. Soc.* **2001**, *123*, 10988.
- (133) Barriocanal, J. A.; Doren, D. J. *J. Am. Chem. Soc.* **2001**, *123*, 7340.
- (134) Armstrong, J. L.; Pylant, E. D.; White, J. M. *J. Vac. Sci. Technol. A* **1997**, *15*, 1146.
- (135) Armstrong, J. L.; Pylant, E. D.; White, J. M. *J. Vac. Sci. Technol. A* **1998**, *16*, 123.
- (136) Wang, G. T.; Mui, C.; Musgrave, C. B.; Bent, S. F. *J. Phys. Chem. B* **2001**, *105*, 12559.
- (137) Widjaja, Y.; Mysinger, M. M.; Musgrave, C. B. *J. Phys. Chem. B* **2000**, *104*, 2527.
- (138) Bozso, F.; Avouris, P. *Phys. Rev. Lett.* **1986**, *57*, 1185.
- (139) Hlil, E. K.; Kubler, L.; Bischoff, J. L.; Bolmont, D. *Phys. Rev. B* **1987**, *35*, 5913.
- (140) Hamers, R. J.; Avouris, P.; Bozso, F. *J. Vac. Sci. Technol. A* **1988**, *6*, 508.
- (141) Dresser, M. J.; Taylor, P. A.; Wallace, R. M.; Choyke, W. J.; Yates, J. T. *Surf. Sci.* **1989**, *218*, 75.
- (142) Fujisawa, M.; Taguchi, Y.; Kuwahara, Y.; Onchi, M.; Nishijima, M. *Phys. Rev. B* **1989**, *39*, 12918.
- (143) Dillon, A. C.; Gupta, P.; Robinson, M. B.; Bracker, A. S.; George, S. M. *J. Vac. Sci. Technol. A* **1991**, *9*, 2222.
- (144) Taylor, P. A.; Wallace, R. M.; Choyke, W. J.; Dresser, M. J.; Yates, J. T. *Surf. Sci.* **1989**, *215*, L286.
- (145) Larsson, C. U. S.; Flodstrom, A. S. *Surf. Sci.* **1991**, *241*, 353.
- (146) Zhou, X. L.; Flores, C. R.; White, J. M. *Surf. Sci.* **1992**, *268*, L267.
- (147) Fattal, E.; Radeke, M. R.; Reynolds, G.; Carter, E. A. *J. Phys. Chem. B* **1997**, *101*, 8658.
- (148) Lee, S. H.; Kang, M. H. *Phys. Rev. B* **1998**, *58*, 4903.
- (149) Takaoka, T.; Kusunoki, I. *Surf. Sci.* **1998**, *413*, 30.
- (150) Queeney, K. T.; Chabal, Y. J.; Raghavachari, K. *Phys. Rev. Lett.* **2001**, *86*, 1046.
- (151) Loh, Z. H.; Kang, H. C. *J. Chem. Phys.* **2000**, *112*, 2444.
- (152) Rignanes, G. M.; Pasquarello, A. *Appl. Phys. Lett.* **2000**, *76*, 553.
- (153) Robinson, D. W.; Rogers, J. W. *Appl. Surf. Sci.* **1999**, *152*, 85.
- (154) Mulcahy, C. P. A.; Carman, A. J.; Casey, S. M. *Surf. Sci.* **2000**, *459*, 1.
- (155) Bailey, P. D.; Morgan, K. M. *Organonitrogen Chemistry*; Oxford University Press: Oxford, 1996.
- (156) McKean, D. C.; Ellis, I. A. *J. Mol. Struct.* **1975**, *29*, 81.
- (157) Bitzer, T.; Richardson, N. V. *Appl. Phys. Lett.* **1997**, *71*, 662.
- (158) Bitzer, T.; Richardson, N. V. *Appl. Surf. Sci.* **1999**, *145*, 339.
- (159) Mui, C.; Han, J. H.; Wang, G. T.; Musgrave, C. B.; Bent, S. F. *J. Am. Chem. Soc.*, accepted.